RSC Advances

PAPER

View Article Online
View Journal | View Issue

Cite this: *RSC Adv.*, 2025, **15**, 13453

Photocatalytic TiO_2/HAP nanocomposite for antimicrobial treatment, promineralization, and tooth whitening†

Ranxu Wang,‡[a] Yanjiu Wang,‡[a] Jiayuan Chen,‡[a] Yue Yin,[a] Nannan Zheng,[b] Mengdi Li,[a] Shuang Zhao,[a] Xu Han,[a] Qiwei Li,[c] Yumei Niu,*[a] Lin Zhang*[a] and Shuang Pan*[a]

Early dental caries and tooth staining are prevalent clinical conditions, so it is of great clinical significance to develop a multifunctional material. Photocatalytic therapies play a significant role in the medical field. However, the use of photocatalytic materials in the dental field is relatively limited. In this study, multifunctional titanium dioxide/nanohydroxyapatite (TiO_2/HAP) nanocomposites were synthesised using a hydrothermal method and investigated for their antibacterial properties, mineralization-promoting effects, tooth whitening capabilities, and biocompatibility. TiO_2 serves as a photocatalyst, facilitating antimicrobial treatment and improving teeth whitening through a photodynamic reaction. HAP, as a mineralization-promoting agent, effectively promotes enamel remineralization following plaque removal. The results of the whitening experiment indicated after treatment by TiO_2/HAP combined with blue light irradiation, the tooth color improved from C4 to A1. In a rat molar model of early caries, TiO_2/HAP effectively removed dental plaque and increased the calcium-to-phosphorus ratio to 1.58, further validating the results of the microhardness test. Meanwhile, TiO_2/HAP nanocomposites demonstrated good biocompatibility *in vivo* and did not significantly alter the oral microbial community. The results indicate that TiO_2/HAP plays a significant role in antimicrobial activity, remineralization, and tooth whitening, offering a novel strategy for the prevention and treatment of early caries and tooth staining.

Received 3rd February 2025
Accepted 11th April 2025

DOI: 10.1039/d5ra00792e

rsc.li/rsc-advances

1 Introduction

Caries is the most prevalent oral disease and the primary cause of tooth pain and tooth loss, significantly impacting the quality of life of patients.[1,2] Plaque is recognized as a major factor in the onset and progression of dental caries and periodontal disease.[3] The primary organism responsible for caries is *Streptococcus mutans* (*S. mutans*),[4] which produces acids by metabolizing carbohydrates found in food. These acids erode the enamel on the surface of the teeth, leading to demineralization and ultimately the formation of cavities. Acid also decreases the resistance of tooth enamel to acid-dissolving calcium, thereby promoting the progression of dental caries.[5] Traditional mechanical plaque removal methods, such as brushing, can be influenced by the operator's technique, potentially leading to chronic damage to the teeth and reduced removal efficiency. Additionally, various types of mouthwashes are commonly used as treatments to control plaque; however, they may have side effects, including tooth staining, irritation, and even the risk of fungal infections in the mouth.[6,7] Dental enamel, the outermost protective layer of the tooth, is generally regarded as non-renewable.[8] Once enamel is damaged, the body cannot repair this damage through its own mechanisms. Therefore, for enamel that has undergone demineralization (early caries), removing plaque can only slow the progression of demineralization and cannot repair the affected enamel. For early caries, current clinical practice relies on the use of fluoride-containing agents, which primarily inhibit bacterial activity and promote remineralization. However, excessive use of fluoride can lead to fluorosis, manifesting as dental fluorosis with white or dark brown spots on the surface of teeth and, in severe cases, potentially affecting bone health.[9] Additionally, fluoride is not only cytotoxic but also causes environmental pollution during its production.[10] In addition, to concerns about caries treatment, tooth whitening has become an important topic for those seeking aesthetic improvement and greater confidence. The color of teeth is affected by a variety of factors, including genetics, diet, smoking, and oral hygiene. Over time, pigments

[a]*The First Affiliated Hospital of Harbin Medical University, Harbin, Heilongjiang 150001, China. E-mail: niuym@hrbmu.edu.cn; cczhlin@163.com; panshuang@hrbmu.edu.cn*

[b]*School of Life Science and Technology, Key Laboratory of Micro-systems and Micro-structures Manufacturing Ministry of Education, Micro/Nano Technology Research Center, Harbin Institute of Technology, Harbin, Heilongjiang Province, 150080, China*

[c]*Harbin Medical University, Harbin, Heilongjiang Province, China*

† Electronic supplementary information (ESI) available. See DOI: https://doi.org/10.1039/d5ra00792e

‡ Authors contributed equally.

can build up on the tooth surface, resulting in yellowing or darkening.[11,12] In addition, the oral cavity serves as a complex bacterial environment, where various bacterial flora interact synergistically to maintain a balanced microecosystem.[13,14] In this balanced environment, the oral flora aids in digestion and helps to combat harmful foreign strains of bacteria.[15] Traditional antibacterial methods, such as the use of mouthwash containing broad-spectrum antibacterial agents, effectively eliminate caries;[16] however, they also indiscriminately kill a large number of beneficial flora in the oral cavity.[17,18] Over time, this can lead to dysbiosis of oral flora and disruption of oral microenvironment, potentially resulting in the development of various oral diseases.[19] Consequently, the pursuit of non-antibiotic alternative treatments has emerged as a crucial focus of contemporary research.

Photocatalysis is a technology that utilizes light energy to excite semiconductor materials,[20,21] generating reactive oxygen species (ROS), which can effectively sterilise bacteria.[22–25] Photocatalytic antimicrobial therapy has attracted much attention due to its controllability and low toxicity, and it is increasingly being investigated as an alternative strategy for the inactivation of pathogenic microorganisms.[26,27] Photocatalytic antimicrobial treatment offers a more gentle alternative to traditional antibiotic therapies.[28] This method uses light to reach areas of the tooth that are difficult to access with traditional techniques, enabling more effective plaque removal.[29–31] As a widely studied photocatalytic material, titanium dioxide (TiO_2) has garnered significant attention in recent years due to its ability to generate highly ROS.[32,33] These ROS can effectively disrupt bacterial cell membranes and organelles, ultimately resulting in bacterial death.[34,35] Furthermore, the strong oxidative properties of ROS enable the decomposition of pigments and organic debris on tooth surfaces, facilitating non-destructive tooth whitening and providing a multifunctional therapeutic effect.[36–38] Photocatalytic antimicrobial technologies developed to date primarily focus on removing plaque and whitening teeth; however, they do not promote tooth remineralization, and their effects on the homeostasis of the oral microenvironment have been infrequently studied. Hydroxyapatite (HAP), the principal component of dental enamel, is widely utilized in restorative dentistry and regenerative medicine.[39,40] It not only exhibits excellent biocompatibility but also contains calcium and phosphorus ions that can effectively repair demineralized tooth enamel, thereby facilitating the treatment of early caries.[41]

In our experiment, TiO_2 was combined with HAP to integrate the advantages of both materials and construct the multifunctional TiO_2-HAP NPs. Hopefully, this NPs not only effectively removed plaque and whiten tooth but also repaired demineralized enamel, resulting in a triple benefit. Additionally, this study investigated the biocompatibility of TiO_2-HAP NPs *in vivo* and their effects on the homeostasis of oral microenvironment (Scheme 1). The aim was to provide a theoretical foundation for the treatment and prevention of caries, as well as to generate a novel idea for the prevention and treatment of oral diseases.

The materials synthesized in this paper exhibit a broader range of properties compared to other titanium dioxide-based and hydroxyapatite-based materials (Table 1). It has been demonstrated that titanium dioxide nanoparticles derived from rosemary and ginger extracts possess anti-inflammatory and antioxidant properties, which enhance the performance of oral materials to a certain degree.[42] Surface-modified TiO_2 dental implants synthesized by Lim *et al.* promote bone regeneration and exhibit antibacterial properties.[43] Other titanium dioxide-based oral materials are also antimicrobial,[44] whitening,[45] and promote mineralization.[46] Currently, hydroxyapatite-based materials are effective in promoting tooth mineralization and

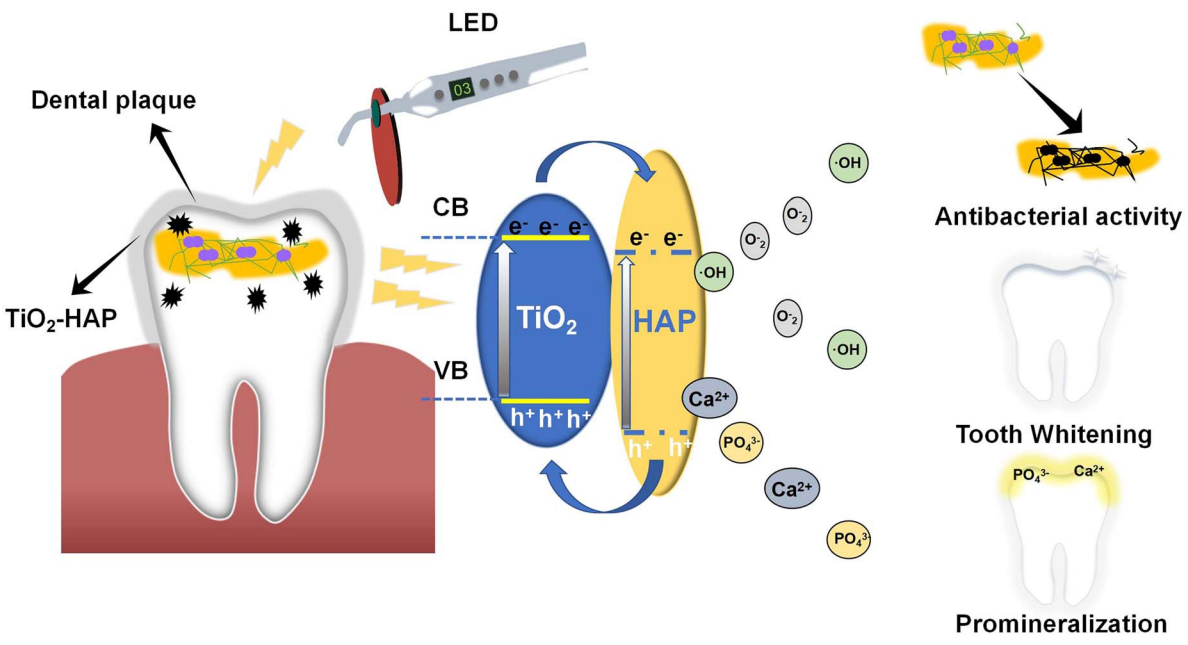

Scheme 1 Mechanism of action of TiO_2-HAP NPs and its antibacterial, mineralization-promoting, and tooth whitening effects.

Table 1 Comparison of different hydrogels[a]

Materials	Antibacterial properties	Tooth whitening	Promineralization
TiO_2 (ref. 44)	✓	✗	✗
TiO_2 nanotubes[45]	✗	✓	✗
TiO_2 nanoparticles[46]	✓	✗	✓
TiO_2 nanotubes[43]	✓	✗	✓
HAP nanoparticles[47]	✗	✗	✓
TiO_2-HAP(this work)	✓	✓	✓

[a] ✓:Have this propertity ✗:Don't have this propertity

bone production. For example, nanohydrogels containing enamel protein peptides and hydroxyapatite nanoparticles, developed by Supian *et al.*, can effectively promote the remineralization of demineralized tooth enamel.[47] This experiment was conducted to determine the optimal method for material synthesis by investigating various conditions, including the titanium-to-calcium molar ratio, reaction pH, and reaction time. The balance between photocatalytic activity (dominated by TiO_2) and biomineralization capacity (dominated by HAP) was investigated by adjusting the ratio of titanium to calcium ions. Under alkaline conditions, the synthesized material exhibits lower solubility, facilitating the formation of a stable solid-phase structure. This environment also enables improved control over the crystalline phase of titanium dioxide, leading to enhanced catalytic activity. The extended reaction time enables the reaction to proceed to completion, allowing for a more uniform distribution of calcium and phosphorus within the synthetic material. In conclusion, the materials synthesized in this paper improve upon the properties of previous similar materials, rendering them more versatile exhibiting antimicrobial, whitening, and promineralization effects and thereby advancing the development of oral materials to some extent.

2 Experimental

2.1 Materials

TiO_2 and HAP were purchased from Hope Bio-Technology; *S. mutans* (ATCC700610) strain was purchased from BeNa Culture Collection; The animals used in this experiment were Sprague-Dawley (SD) male rats (8 weeks old, weighing about 200–250 g) and Kunming male mice (4 weeks old, 20–30 g), which were provided by the Animal Experimentation Centre of Medical University of the First Affiliated Hospital of Harbin Medical University. All animal experiments were conducted in accordance with the ARRIVE guidelines 2.0 and approved by the Institutional Animal Care and Use Committee of Animal Experimentation Centre of Medical University of the First Affiliated Hospital of Harbin Medical University (Protocol No. 2023116).

2.2 Preparation and characterization of TiO_2-HAP NPs

The synthesis of TiO_2-HAP NPs was conducted using a hydrothermal method.[48] Firstly, hydroxyapatite nanoparticles were dissolved in a dilute hydrochloric acid solution (0.1 mol L^{-1}) with stirring. Then, TiO_2 nanoparticles were introduced to form three suspension groups with titanium-to-calcium molar ratios of 2 : 1, 1 : 1, and 1 : 2, respectively. Ammonia solution was added to the suspension, and the pH was adjusted to 11. The mixture was then heated to 90 °C and stirred for 6 h. The precipitate obtained after filtration was dried to yield TiO_2-HAP powder. The synthesized samples were analyzed using UV-vis spectroscopy and fluorescence spectroscopy to assess the radical generation capability of TiO_2-HAP. In a similar manner, we employed a 1 : 2 molar ratio of TiO_2 to HAP, adjusting the pH to 7, 9, 11 and 13 to obtain four sets of TiO_2-HAP powders. Finally, we selected the TiO_2 and HAP with a 1 : 2 molar ratio, adjusted the pH to 11, heated to 90 °C, and stirred for 1, 2, 4, and 6 h, respectively, to obtain four sets of TiO_2-HAP powders. The synthesized samples were characterized by Scanning electron microscopy (SEM) and Transmission Electron Microscopy (TEM) for morphological analysis. The chemical composition and structural properties were further verified by X-ray Photoelectron Spectroscopy (XPS), Fourier Transform Infrared Spectroscopy (FTIR), and X-ray Diffraction (XRD) analyses.

2.3 Free radical testing

The hydroxyl radicals (·OH) generated by TiO_2-HAP photocatalysis exhibit antibacterial properties by oxidizing and damaging bacterial cell membrane lipids and proteins. This study systematically confirmed the efficient production of ·OH under UV irradiation through a multi-dimensional experimental approach: Firstly, we determine the band gap of the synthesized sample using Tauc plot, which is derived from the UV-vis diffuse reflectance spectrum (DRS). Subsequently, UV-vis absorption spectroscopy and fluorescence intensity measurements validated its UV light-harvesting capability. Electron spin resonance (ESR) spectroscopy verified the photocatalytic-dependent generation of ·OH, and finally, the terephthalic acid (TA) fluorescence probe method quantitatively demonstrated the ·OH yield.

2.4 Microhardness test

Thirty enamel blocks were initially prepared and immersed in 100 mL of demineralization solution (pH = 5) for 48 h to obtain demineralized lesions. Subsequently, the enamel blocks were randomly divided into five groups: TiO_2-HAP group, TiO_2-HAP + LED group, sodium fluoride (NaF) group, untreated enamel group; demineralized enamel group, with six samples in each group. The drug concentrations for the TiO_2-HAP group, and TiO_2-HAP + LED group were set at 1.5 mg mL^{-1}, while the

concentration of NaF was 20 mg mL^{-1}. The enamel blocks were immersed in each group of drugs for 10 min, while the TiO_2-HAP + LED was simultaneously exposed to blue LED light twice daily for 15 days. Hardness tests were conducted using a Vickers hardness tester, and a microscope was employed to observe the indentations and measure their diagonal lengths. The hardness value was calculated using the formula for Vickers hardness: Vickers hardness (HV) = 1.8544 × (load/dent surface area).

2.5 TiO_2-HAP NPs for tooth enamel whitening

Six isolated teeth were collected. The periodontal membrane and other soft tissues on the surface of the teeth were removed using a scalpel. The surfaces of the teeth were polished with 600, 800, and 1000 mesh silicon carbide sandpaper and then stored in deionized water at 4 °C for later use. To prepare the staining solution, 6 g of black tea was steeped in 100 mL of boiling water, sterilized under UV light for 20 min, and then filtered and set aside. The teeth were immersed in a staining solution for one week in an incubator at 37 °C. The staining solution was stirred once daily and replaced every two days. The teeth were rinsed with deionized water to remove any residual staining agents from the tooth surface. 0.5 mL of TiO_2-HAP mixture was dropped onto the surface of stained enamel, and light treatment was applied for 10 h. Every 2 h, the tooth color was compared with the Vita color guide and photographed to observe the change in tooth color before and after treatment. Then, twelve stained premolar teeth were randomly divided into 2 groups ($n = 6$). In each group, 0.5 mL of a liquid solution containing a concentration of 1.5 mg mL^{-1} TiO_2-HAP was applied to the enamel surface, and each group was treated for 10 hours. After 10 hours, changes in tooth color were assessed using the CIELAB color space. The values of L, a and b for the treated teeth were measured using a colorimeter. In this context, L indicates the brightness of the sample on a scale from black (0) to white (100), while a represents the green-red coordinates, and b denotes the blue-yellow coordinates. The teeth were placed on a neutral gray background, and measurements were taken by placing the tip of the colorimeter in contact with the middle third of the tooth surface, ensuring it was perpendicular to the surface. The L, a, and b values of the stained teeth were recorded by the colorimeter as baseline values.

2.6 Cytotoxicity assay

The cytotoxicity of TiO_2-HAP NPs toward dental pulp stem cells (DPSCs) was assessed using the 3-(4,5-dimethylthiazol-2-yl)-2,5-diphenyltetrazolium bromide (MTT) assay. Briefly, DPSCs were seeded into 96-well plates at a density of 5×10^3 cells per well and cultured at 37 °C under 5% CO_2 for 24 h. After incubation, the culture medium was replaced with fresh medium containing varying concentrations of TiO_2-HAP (0, 0.2, 0.4, 0.6, 0.8, 1, 1.5 mg mL^{-1}). Control group refers to the group without TiO_2-HAP. Cells were further incubated for 24 h. Subsequently, 20 μL of MTT solution was added to each well, followed by 4 h of incubation at 37 °C. The formed formazan crystals were dissolved by adding 150 μL of dimethyl sulfoxide (DMSO) to each well after careful removal of the medium. The plates were gently agitated for 10 min in the dark to ensure complete dissolution.

The optical density (OD) of each well was measured at 570 nm. Cell viability (%) was calculated using the formula:

$$\text{Viability (\%)} = (\text{OD sample-OD blank/OD control-OD blank}) \times 100\%$$

2.7 Antibacterial experiment

To determine the optimal titanium-to-calcium molar ratio of the TiO_2-HAP, we conducted antimicrobial assay. Bacterial suspensions (*S. mutans*) were co-cultured with -HAP at different titanium-to-calcium molar ratios (2 : 1, 1 : 1, 1 : 2) for 16 hours, followed by measurement of the OD_{600} values of the bacterial suspensions. Then, based on the antibacterial effects mentioned above, we select the optimal titanium-calcium molar ratio material for bacterial plate coating experiments to further verify the antibacterial effect.

2.8 *In vivo* safety and efficacy assessment of TiO_2-HAP NPs

2.8.1 *In vivo* safety assessment in mice. Twelve Kunming male mice were selected, acclimatized, and fed for 1 week at a temperature of (25 ± 2) °C with 55% ± 5% humidity and alternating dark cycles. During this period, the mice had ad libitum access to distilled water and sterile food. The drug was administered by gavage. The mice were randomly divided into 2 groups ($n = 6$): control group and TiO_2-HAP group. The mice were weighed prior to gavage. Saline was administered to control group at a dosage of 0.1 mL per 10 g of body weight, while the TiO_2-HAP group received a TiO_2-HAP suspension with a concentration of 1.5 mg mL^{-1}, also based on 0.1 mL per 10 g of body weight. The drug was administered *via* gavage once daily for 2 weeks, and the daily body weight of the mice was recorded. At the end of the gavage period, 3 mice from each group were randomly selected for routine blood analysis and assessment of biochemical indices. Subsequently, all mice were euthanized and dissected; their hearts, livers, spleens, kidneys, and lungs were immersed in 4% formaldehyde solution for fixation, embedded in paraffin wax, sectioned, and stained with hematoxylin and eosin (HE). The histopathological changes in the tissues were examined using a light microscope.

2.8.2 Establishment of an early caries model for rat molar teeth. *S. mutans* were applied to the buccal surface of the mandibular molars of rats using a resin adhesive stick, while phosphate-buffered saline (PBS) was applied to the buccal surface of the mandibular molars in the negative control group. The bacteria were inoculated once daily for 15 consecutive days. On the fifth day of bacterial inoculation, a sterile cotton swab was used to collect a sample from the buccal surface of the mandibular molar of the rat, which was then transferred to BHI solid medium and incubated anaerobically at 37 °C for 48 h to confirm the formation of *S. mutans* colonization. During the modeling period, the rats were fed a high-sugar diet consisting of Diet 2000 caries chow and a 5% sucrose solution. After modeling, sodium pentobarbital was administered, and

anesthesia was induced *via* isoflurane. Once the anesthesia took effect, rat mandibular specimens were obtained using sterile surgical instruments. The jaws were fixed in 4% paraformaldehyde. Routine dehydration, embedding, and gold sputter coating were performed. The morphology and elemental distribution of the composite were examined by SEM (Scanning Electron Microscopy) and TEM (Transmission Electron Microscopy), while its phase composition was confirmed by XRD. Chemical bonding and surface states were further investigated using XPS (X-ray Photoelectron Spectroscopy) and FTIR (Fourier Transform Infrared Spectroscopy).

2.8.3 *In vivo* effectiveness evaluation of TiO_2-HAP NPs. The animals used in this experiment were SD male rats, aged 8 weeks and weighing approximately 200 to 250 grams. The rats were randomly divided into 4 groups ($n = 6$). Negative control group: SD rats were fed distilled water and normal food for 30 days without any other treatments. Positive control group: SD rats were fed a high-glucose diet for 15 days following the establishment of an early tooth decay model, without any additional treatment. TiO_2-HAP treatment group: After the establishment of the early caries model for molar teeth, SD rats were fed a high-sugar diet for 15 days. During this period, a TiO_2-HAP NPs suspension at a concentration of 1.5 mg mL^{-1} (based on our previous study) was applied to the buccal side of the rats' molar teeth using ethylene oxide-sterilized resin bonding rods. A light was then shone on the application site for 5 min, once daily. TiO_2-HAP prevention group was established in which a bacterial solution containing 1×10^8 CFU mL^{-1} of *S. mutans* was applied to the buccal side of the mandibular molars of healthy rats. After a period of 12 h, a suspension of TiO_2-HAP NPs at a concentration of 1.5 mg mL^{-1} was applied, followed by light irradiation for 5 min. This cycle was repeated once daily, and the entire experimental duration lasted for 15 days. During this period, a high-sugar diet was maintained.

At the end of the experiment, disposable sterile throat swabs were used for multiple collections and mixing to gather oral flora from each group, once in the morning and once in the afternoon. The swabbing sites were the sublingual mucous membrane of oral cavity, without contacting with the experimental teeth until the saliva had completely moistened the pharyngeal swabs. Subsequently, the swabs were placed into sterile EP tubes and stored at −20 °C. Six samples were collected from each group, DNA extraction from the buccal mucosa of rats was performed using an E.Z.N.A™ Mag-Bind Soil DNA Kit (Omega, M5635-02, USA), following the manufacturer's instructions. PCR amplification was conducted following DNA extraction. Two pairs of specific 16S rRNA gene amplification primers (PAGE purified) were utilized: the upstream primer 341F (5′-CCTACGGGGNGGCWGCAG-3′), and downstream primer 805R (5′-GACTACHVGGGGTATCTAATCC-3′) to amplify the V3–V4 of 16S rRNA gene. The PCR reaction system consisted of the following components: microbial DNA (10 ng μL^{-1}) - 2 μL, upstream primer (10 μM) - 1 μL, downstream primer (10 μM) - 1 μL, and 2×Hieff® Robust PCR Master Mix - 15 μL. The plate was sealed and PCR performed in a thermal instrument (Applied Biosystems 9700, USA) using the following program: 1 cycle of denaturing at 95 °C for 3 min, first 5 cycles of denaturing at 95 °C for 30 s, annealing at 45 °C for 30 s, elongation at 72 °C for 30 s, then 20 cycles of denaturing at 95 °C for 30 s, annealing at 55 °C for 30 s, elongation at 72 °C for 30 s and a final extension at 72 °C for 5 min. We used Hieff NGS™ DNA Selection Beads (Yeasen, 10105ES03, China) to purify the free primers and primer dimer species in the amplicon product. Samples were delivered to Sangon BioTech for library construction using universal Illumina adaptor and index. USEARCH was used for the clustering of operational taxonomic units (OTUs). Bioinformatic analysis was performed using Mothur, the following analyses were performed using the Sangong biotech Cloud Platform. At the end of the experiment, SD rats were euthanized, and mandibular specimens were obtained using sterile surgical instruments to excise the soft tissues of the jaws. The jaws were rinsed three times with PBS and subsequently fixed in 4% formaldehyde. SEM and EDS were employed to evaluate the surface morphology, bacterial distribution, demineralization, and elemental composition of the rat molar teeth.

2.9 Statistical analysis

Data were statistically analyzed using GraphPad Prism 7 software, and the values are expressed as the mean ± standard deviation (SD), using *t*-test to analyze, with asterisks (*) indicating statistically significant differences between values (*P < 0.05, **P < 0.01, ***P < 0.001).

3 Results and discussion

3.1 Effect of various synthesis conditions on the properties of TiO_2-HAP NPs

3.1.1 Molar ratio of various titanium ions to calcium ions. In this experiment, TiO_2-HAP NPs with titanium-to-calcium molar ratio of 2 : 1, 1 : 1, and 1 : 2 were synthesized. SEM images and elemental analysis results indicate that the distribution of titanium and calcium elements is relatively uniform (Fig. S1a–c†).

3.1.2 Various of pH values and times. During the hydrothermal synthesis, the pH of each experimental group was adjusted to 7, 9, 11, and 13, respectively. The resulting TiO_2-HAP NPs was morphologically observed using SEM and analyzed elementally through EDS. As shown in Fig. S2,† the synthesized TiO_2-HAP NPs exhibited optimal morphological stability when the pH was adjusted to 11, resulting in a more uniform distribution of calcium and phosphorus elements within the materials. Meanwhile, the calcium and phosphorus element distribution of the product after stirring for 6 h is more uniform (Fig. S3†). Additionally, the fit between atomic molar ratios of the products and the original reactant ratios achieved a high degree of accuracy. These findings suggest that an appropriate pH and acting time are crucial for optimizing the synthesis process and enhancing the final properties of TiO_2-HAP NPs.

3.2 Characterization of TiO_2-HAP

The successful synthesis of TiO_2-HAP NPs (titanium-to-calcium molar ratio of 1 : 2) was confirmed through comprehensive material characterizations. TEM analysis revealed the formation

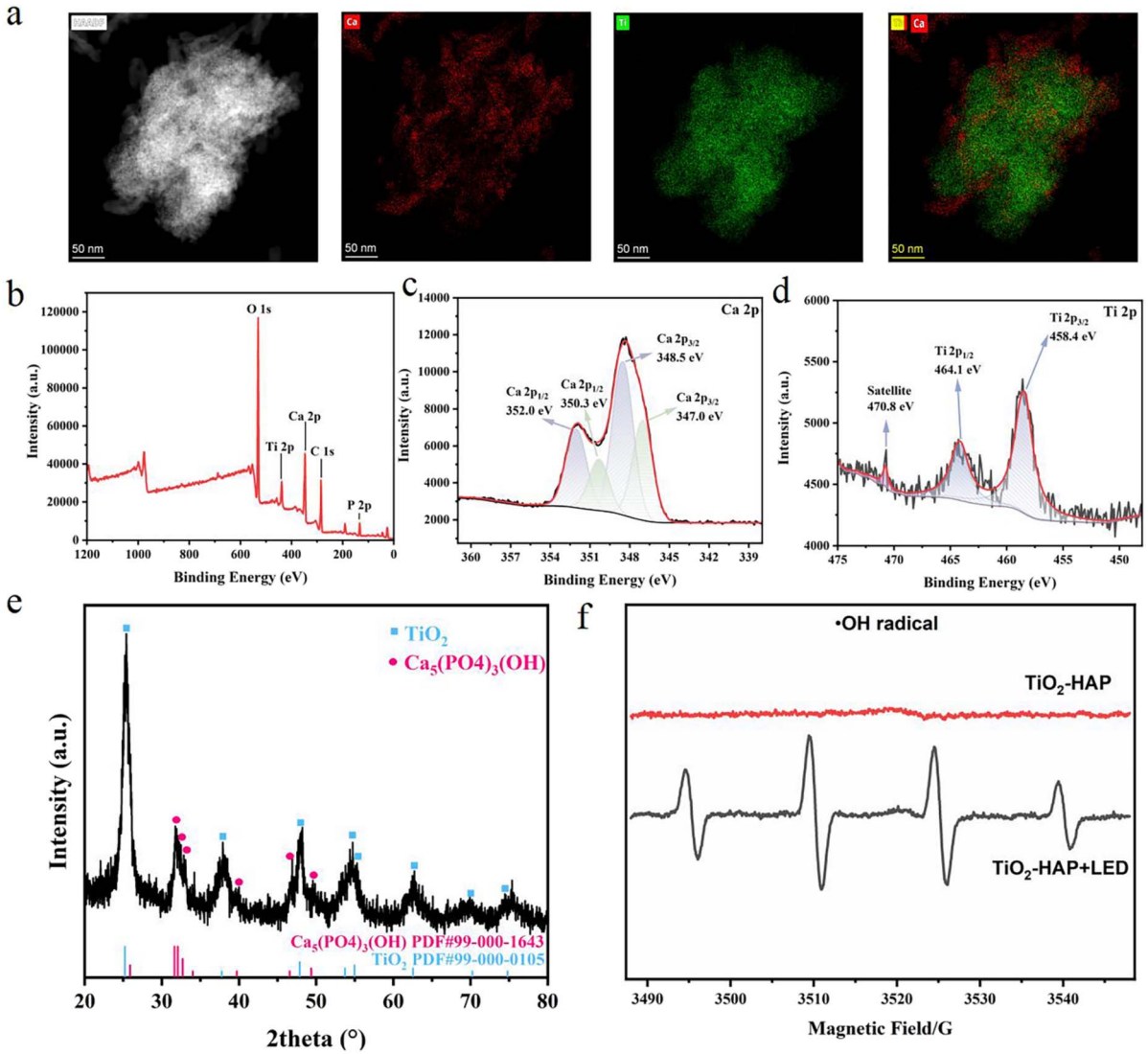

Fig. 1 (a) TEM image showing the overall morphology and elemental analysis of TiO_2-HAP NPs. (b–d) XPS results of TiO_2-HAP NPs. (e) XRD results of TiO_2-HAP NPs. (f) ESR results of TiO_2-HAP NPs.

of TiO_2-HAP NPs (Fig. 1a). The chemical composition and structural properties were further verified by XPS, FTIR, and XRD analyses. The XPS analysis confirmed the presence of titanium (Ti) and calcium (Ca) on the sample surface, suggesting the formation of a TiO_2-HAP composite material. The peaks at 348.5 eV and 350.3 eV confirm the presence of Ca^{2+} in the HAP lattice, while the additional peaks at 347.0 eV and 352.0 eV suggest interactions with TiO_2, leading to variations in the binding energy.[49] The Ti 2p spectrum displayed characteristic peaks at 458.4 eV (Ti 2p3/2) and 464.1 eV (Ti 2p1/2), indicating that titanium primarily exists in the Ti^{4+} oxidation state, typical of TiO_2.[50] These findings suggest that the material comprises a TiO_2-HAP composite (Fig. 1b–d). In the FTIR spectrum, the broad absorption peak of TiO_2 in the range of 800–450 cm^{-1} corresponds to the stretching vibration of Ti–O bonds.[51] For HAP, the absorption peaks at 962 cm^{-1} and 602 cm^{-1} are assigned to the stretching vibration and triply degenerate vibration modes of P–O bonds in PO_4^{3-}, while the peaks at 1091 cm^{-1} and 632 cm^{-1} correspond to the stretching vibration of P–O–H bonds.[52] In the FTIR spectrum of TiO_2/HAP nanoparticles, characteristic absorption peaks of HAP are observed at 566, 602, 632, 962, 1033, and 1091 cm^{-1},[53] whereas the characteristic peaks of TiO_2 appear in the range of 800–450 cm^{-1} (Fig. S4†). The coexistence of these distinctive peaks from both TiO_2 and HAP in the composite spectrum demonstrates the successful incorporation of TiO_2 into the HAP. XRD patterns displayed characteristic diffraction peaks at 2θ = 31.65°, 37.77°, and 47.87°, matching well with the standard patterns of anatase TiO_2 and hydroxyapatite (Fig. 1e).

3.3 Hydroxyl radicals tests

Firstly, we draw the ROS generation mechanism and elaborate the pathways herein (Scheme 2). The mechanism involves the excitation of electrons from the valence band to the conduction band, leading to the formation of electron–hole pairs. These

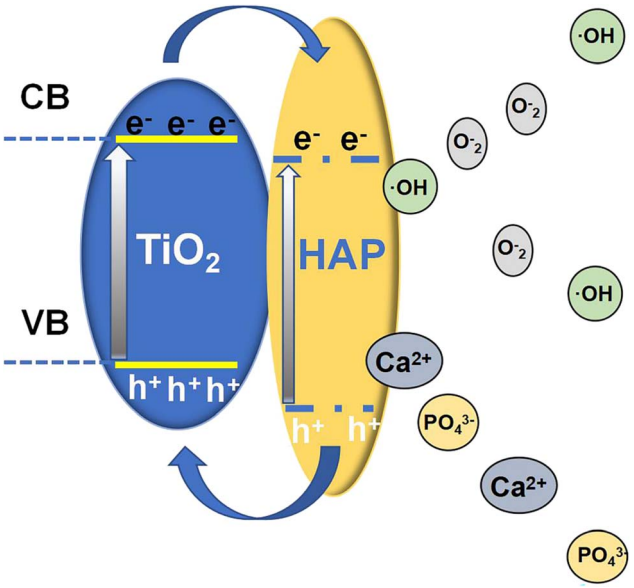

Scheme 2 ROS generation mechanism and elaborate the pathways herein.

charge carriers subsequently react with O_2 and H_2O to generate $\cdot O_2^-$ and ·OH, respectively. The photocatalytic performance of TiO_2-HAP nanocomposites was systematically evaluated through multi-technique characterization. First, the bandgap energies of samples with varying titanium-to-calcium molar ratios (1 : 2, 2 : 1, and 1 : 2) were determined *via* Tauc plot derived from UV-vis diffuse reflectance spectroscopy (DRS), revealing values of 3.22 eV, 3.27 eV, and 3.3 eV, respectively (Fig. S5a†). The lowest bandgap of the 1 : 2 sample indicates enhanced visible-light responsiveness due to reduced energy requirements for electron excitation. This was corroborated by UV-vis absorption spectra, where the 1 : 2 nanocomposite exhibited significantly stronger light absorption beyond 400 nm compared to other ratios (Fig. S5b†). Fluorescence intensity measurements (350–550 nm) further demonstrated that the 1 : 2 ratio sample generated the highest concentration of hydroxyl radicals (·OH) under illumination (Fig. S5c†). ESR spectroscopy demonstrated the TiO_2-HAP composite effectively promotes free radical generation under light exposure. This enhanced photocatalytic activity makes the TiO_2-HAP NPs particularly suitable for applications in dental antibacterial treatment and tooth whitening (Fig. 1f). Quantitative analysis using TA fluorescence probe confirmed time-dependent ·OH production (Fig. S5d†).

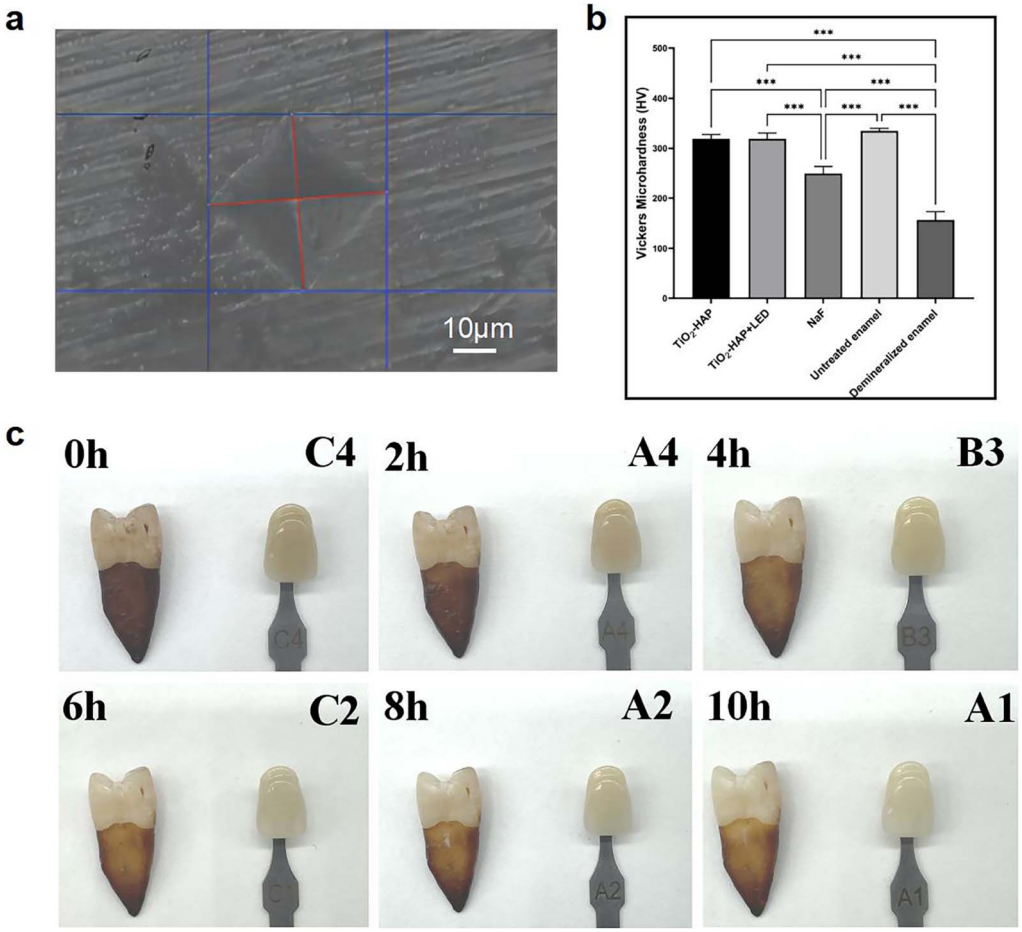

Fig. 2 (a) Microhardness testing image of enamel. (b) Microscratch hardness test results of enamel for each group, ***$p < 0.001$. (c) Evaluation of the tooth whitening effect of TiO_2-HAP NPs.

Collectively, these results highlight the superior photocatalytic activity of the 1 : 2 TiO_2-HAP nanocomposite, making it a promising candidate for dental applications such as antibacterial therapy and tooth whitening through ·OH-mediated oxidative mechanisms.

3.4 Microhardness test results

Microhardness testing image of enamel is shown in Fig. 2a, and S6† shows the specific test values for one trial. The results of the enamel microhardness tests for each group are presented in Fig. 2b and Table 1. The microhardness values were as follows: 318.89 ± 8.86 for TiO_2-HAP group, 318.93 ± 11.56 for TiO_2-HAP + LED group, 249.39 ± 13.96 for NaF group, 344.57 ± 5.52 for Untreated enamel group, and 156.08 ± 16.82 for Demineralized enamel group. The results indicated that the differences in enamel microhardness values were statistically significant ($P < 0.001$), with the exception of the TiO_2-HAP and TiO_2-HAP + LED groups. Furthermore, the results demonstrated that the TiO_2-HAP NPs significantly enhanced the microhardness of demineralized enamel, outperforming NaF.

3.5 Whitening effect of TiO_2-HAP NPs on dental enamel

As shown in Fig. 2c, the tooth whitening effect of TiO_2-HAP NPs was assessed in this experiment by measuring the change in the teeth color shade scale. The color shade of the TiO_2-HAP NPs with light treatment for 10 h changed from C4 to A1, representing an improvement of 11 shades. The *L*, *a* and *b* values before and after tooth whitening are presented in Fig. S9.† The TiO_2-HAP group exhibited an increase in *L* values and a decrease in both *a* and *b* values then before. The quantitative analysis of the measurements using the CIELAB color space corroborated the results shown in Fig. S7.† The results indicate that TiO_2-HAP NPs exhibited a significant tooth whitening effect under blue light irradiation.

3.6 Antibacterial experiment

To investigate the antibacterial properties of TiO_2-HAP with varying titanium-to-calcium molar ratios, bacterial optical density (OD) measurements were conducted. The results revealed that the TiO_2-HAP nanocomposite with a titanium-to-calcium molar ratio of 1 : 2 exhibited superior antibacterial efficacy (Fig. S8†). Subsequently, a bacterial colony-forming unit (CFU) assay was performed using the 1 : 2 ratio sample. Compared to control groups, the TiO_2-HAP + LED group demonstrated significantly fewer bacterial colonies, further confirming its antimicrobial activity under light exposure.

3.7 Biocompatibility assessment

The biocompatibility of the material is crucial. Firstly, we conducted cytotoxicity testing on the material, and the results showed that concentrations ranging from 0 to 1.5 mg mL^{-1} did not show significant toxicity to cells compared to the control group (Fig. S10†). Afterward, we measured the body weight of the mice. As shown in the Fig. 3a, following the drug gavage experiment, the body weights of mice in both TiO_2-HAP group and control group increased steadily, exhibiting a similar growth trend. There was no statistically significant difference between the two groups, indicating that TiO_2-HAP NPs had no significant effect on the living condition of mice. To further investigate the biocompatibility of TiO_2-HAP NPs, HE staining

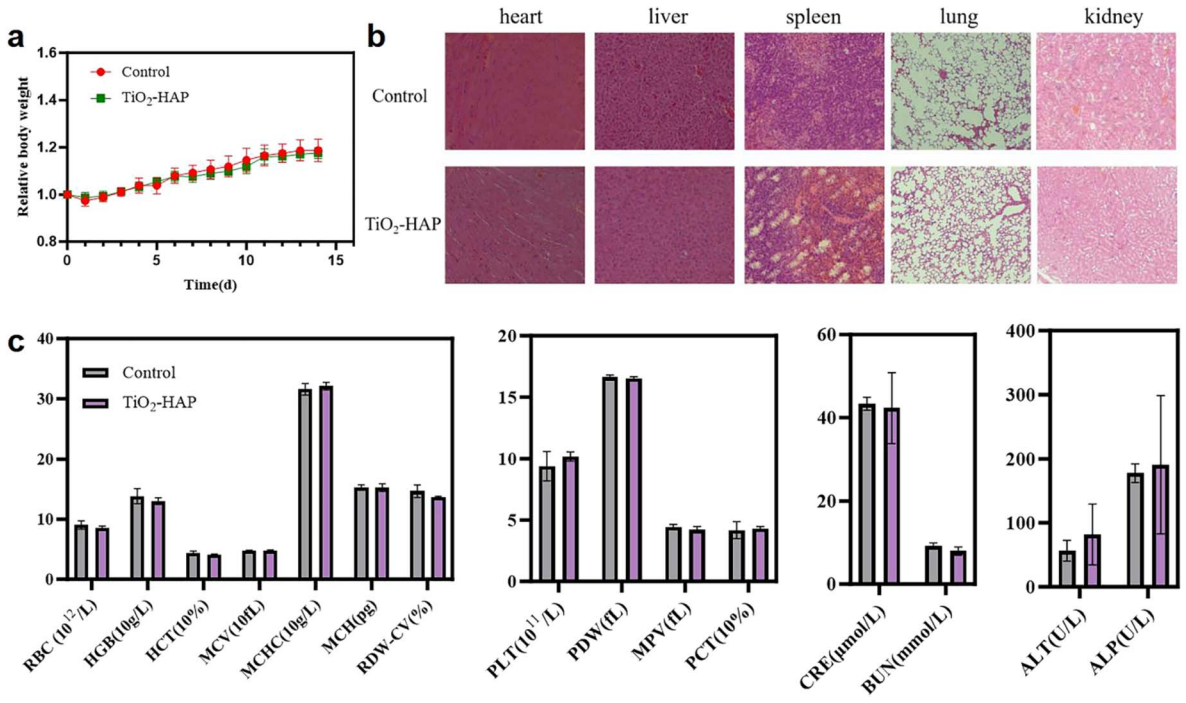

Fig. 3 (a) Weight change chart of each group of mice. (b) H and E staining results of major organs in mice of each group. (c) Hematological test results of mice in each group.

was performed on the vital organs of the mice in this experiment. Compared to control group, the mice of TiO_2-HAP group did not exhibit significant inflammatory reactions in the tissues of any organ (Fig. 3b), indicating that TiO_2-HAP does not possess notable toxicity to vital organs. The results of routine blood tests conducted after gavage in mice are shown in Fig. 3c. Both groups exhibited values within the normal range for hematological and biochemical indices, and no significant differences were observed. Based on the aforementioned indicators, we can know that TiO_2-HAP NPs demonstrated good biocompatibility *in vivo*.

3.8 Successful establishment of an early caries model for rat molar teeth

On the fifth day of modeling, a sterile cotton swab was used to collect a sample from the buccal side of the rat's mandibular molar. This sample was then placed in a liquid medium for 24 h, followed by coating with BHI solid medium and incubating anaerobically at 37 °C for 48 h. Fig. S11† showed a significant number of *S. mutans* colonies in the Petri dish, indicating that the *S. mutans* had successfully colonised. The rats were euthanized after the 15th day of modeling, and sterile surgical instruments were used to collect specimens of the rat mandibles. The result of microscopy is presented in Fig. 4a, scattered blocks of chalky enamel areas (indicated by red arrows) were observed in the buccal portion of the molar teeth of the rats. SEM image and calcium-to-phosphorus ratio (1.65) of normal enamel are shown in Fig. 4b, it indicates that the surface of the control rat molar is smooth and flat. Fig. 4c shows a significant presence of bacterial biofilms covering the surfaces of rat molar teeth in the modelling group, and Fig. 4d depicts numerous scattered fissures on the enamel surface of rat molar teeth in the uncovered area, with a substantial distribution of bacteria surrounding these fissure. Elemental analysis revealed that the calcium-to-phosphorus ratio of rat molar teeth in the modeling group decreased to 1.40. Collectively, these findings indicate that an early caries model of rat molar teeth was successfully established in the rats.

3.9 Evaluation of the antibacterial and pro-mineralisation properties of TiO_2-HAP NPs on rat molar teeth

Fig. 5 are the SEM images and elemental analyses of rat molar teeth after treatment of each group. As shown in Fig. 5a, the surface of rat molar teeth in negative control group was smooth and flat, with a calcium-to-phosphorus ratio of approximately 1.67. Fig. 5b illustrates an image of rat molar teeth from positive control group, which demonstrates ongoing proliferation of *S. mutans*, continued demineralization of the enamel, and a reduction in the calcium-to-phosphorus ratio to 1.03 after 15 days of high-glucose feeding following modeling. In contrast, the image of the TiO_2-HAP treatment group (Fig. 5c), reveals that the plaque on the surface of the rat molar teeth has been completely removed, and scattered fissures remain visible on the surface, the elemental ratio of calcium to phosphorus has been restored and increased to 1.58, almostly approaching the normal level of enamel mineralisation. In the TiO_2-HAP prevention group, there were no visible bacteria on the surface of the molars,and no significant enamel damage was observed. Additionally, the calcium-to-phosphorus ratio increased to 1.80 (Fig. 5d). Overall, the animal study has demonstrated that TiO_2-HAP exhibits good antibacterial properties and effectively restores demineralized enamel. Furthermore, it provides good preventive effects on enamel in a caries-inducing environment.

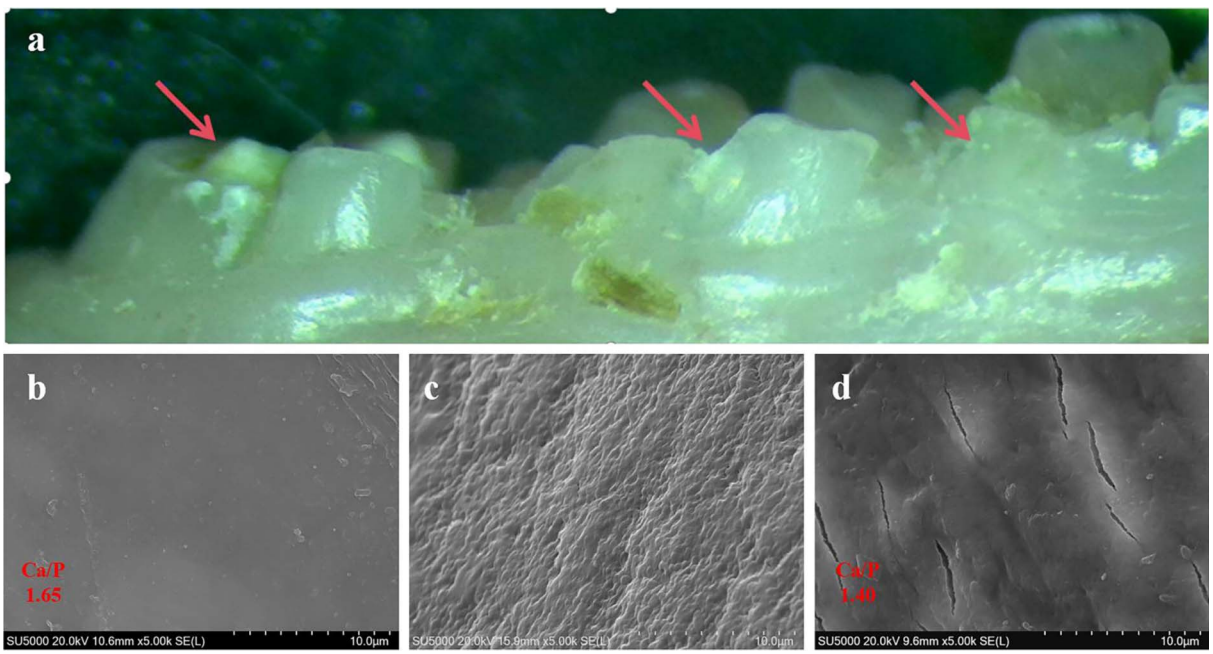

Fig. 4 (a) Microscopic observation of rat molar (red arrows indicate demineralized areas). (b) SEM image and elemental analysis of normal enamel. (c) SEM image of bacteria on the enamel surface of Modeling group. (d) SEM image and elemental analysis of Modeling group.

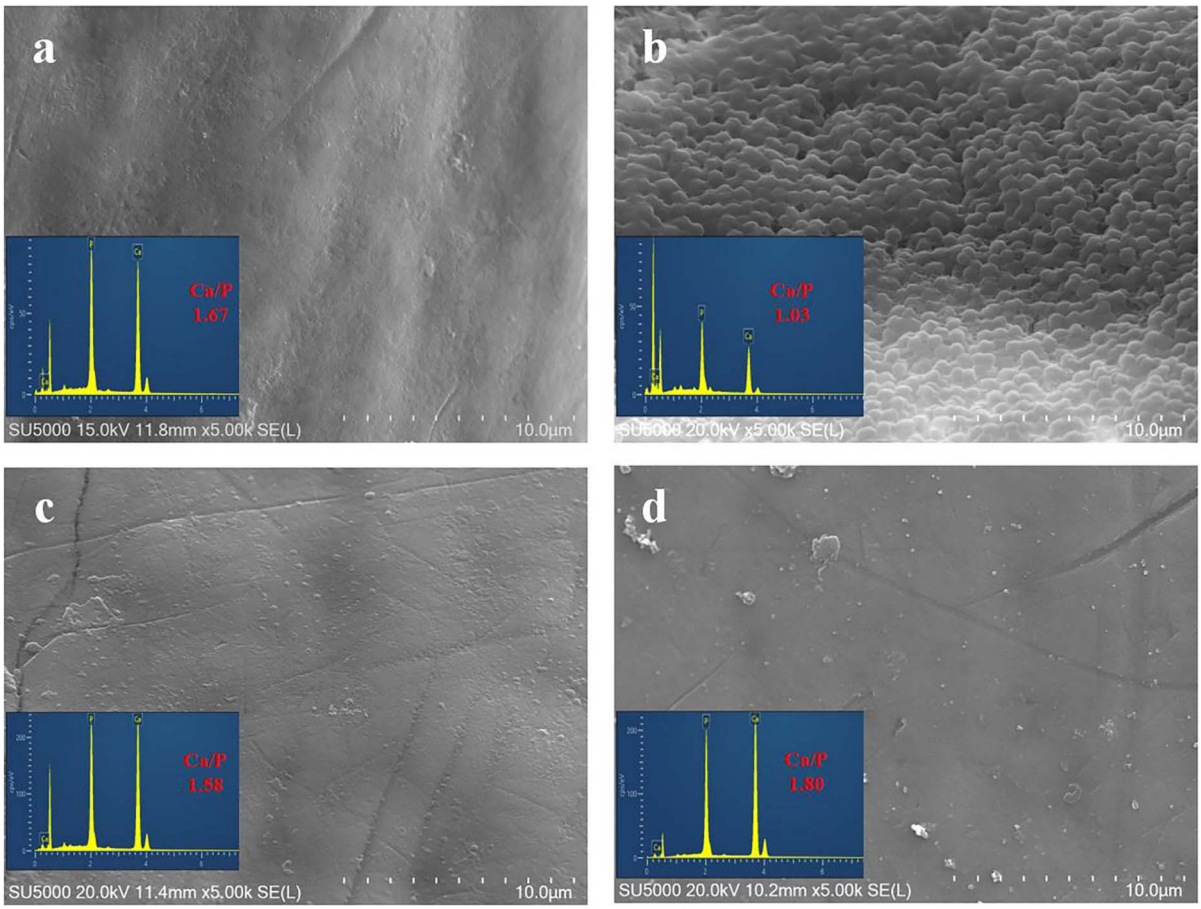

Fig. 5 SEM images and elemental analysis of (a) negative control group, (b) positive control group, (c) TiO_2-HAP treatment group and (d) TiO_2-HAP prevention group.

3.10 Evaluation of the effect of TiO_2-HAP NPs on the oral bacterial microenvironment in rat

As shown in Fig. 6a, α-diversity analysis revealed a significant increase in the abundance of oral microbial species in positive control group at 30 days. Additionally, the interspecies differences increased, indicating that the oral flora of the rats became progressively dysbiotic following the implantation of *S. mutans*. There was no statistically significant difference between the two groups treated with TiO_2-HAP NPs (TiO_2-HAP treatment group and TiO_2-HAP prevention group) and the negative control group ($P > 0.05$). This indicates that the diversity of the oral flora in rats could be significantly regulated, and the interspecies differences could be reduced through the intervention of TiO_2-HAP NPs. Fig. 6b shows the composition of the microbial community and the distribution of dominant bacteria in the different groups. In all groups, *g-Rothia*, *g-Rodentibacter*, and *g-Streptococcus* were the main dominant bacteria. The statistical analysis comparing negative control group and the TiO_2-HAP treatment group is presented in Fig. 6c. The results indicated that none of the three bacterial species showed statistically significant differences between the two groups ($P > 0.05$). This finding suggests that the three dominant bacteria in the oral microenvironment were not influenced by the treatment with TiO_2-HAP NPs. Consequently, it can be inferred that TiO_2-HAP NPs had minimal interference with the microbial community and demonstrated good biocompatibility. The β-diversity results are shown in Fig. 6d, where principal coordinate analysis (PCoA) was conducted using the bray curts distance. Ellipses represent 95% confidence intervals. The results revealed significant differences in the spatial distribution of microbial community composition among each group. Negative control group were closely clustered and positioned in the upper right quadrant of the graph, exhibiting typical characteristics of a healthy oral ecological community. Compared to the negative control group, the samples from Modeling group and positive control group exhibited significant deviations and clustered in distinct regions on the left side. This suggests that the inoculation of *S. mutans* resulted in significant changes in the oral microbiota. The TiO_2-HAP treatment group highly overlapped with negative control group, and the distribution of communities was more concentrated. This indicates that TiO_2-HAP treatment did not significantly disrupt the structure of the oral microecological community. The TiO_2-HAP prevention group slightly overlapped with the Modeling group but primarily deviated from it. This in-dicates that the preventive treatment maintained a protective and corrective effect on the oral microenvironmental homeostasis of the rats, despite the

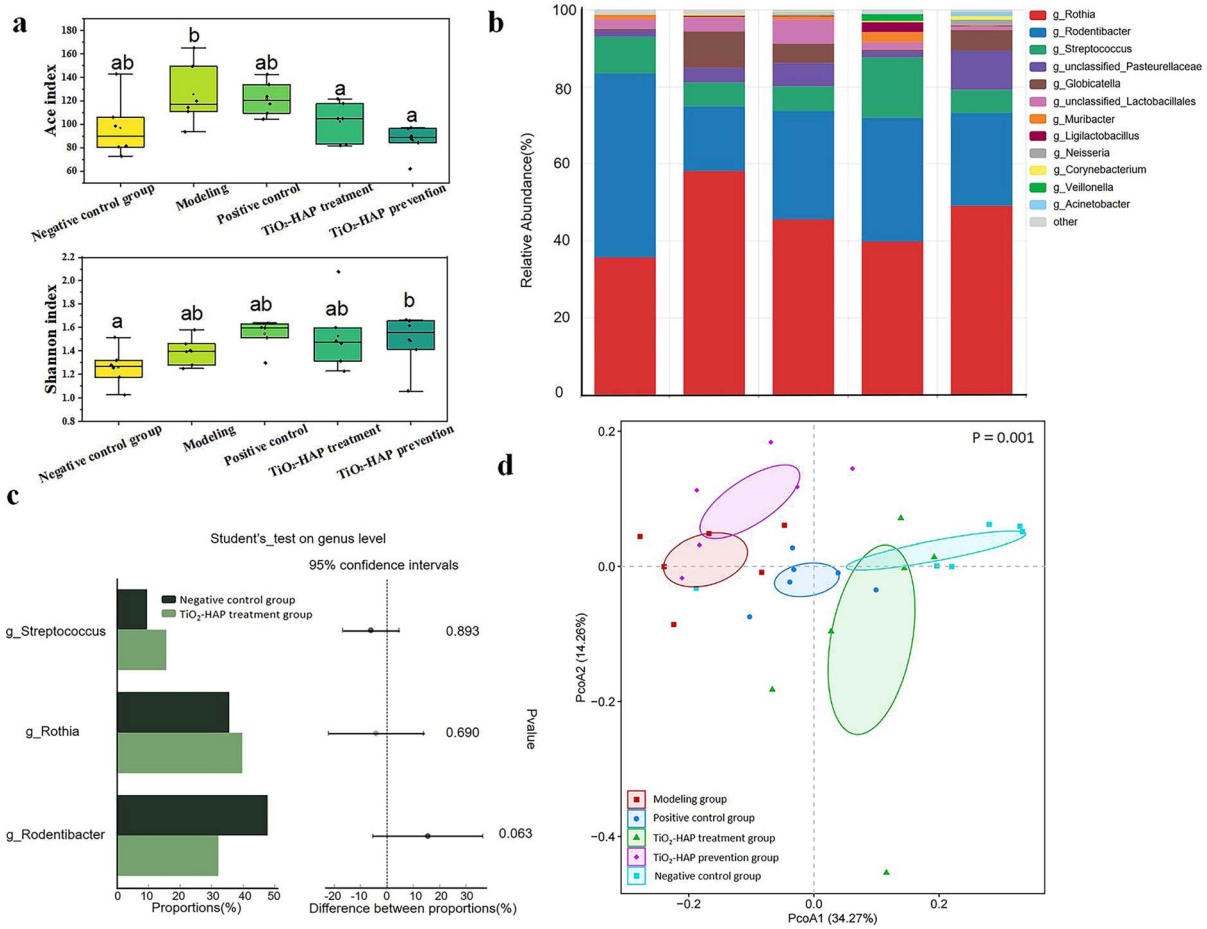

Fig. 6 (a) Ace index and Shannon index of each group. (b) The composition of microbial communities and the distribution of dominant bacteria of each group. (c) Statistical analysis of the differences between negative control group and TiO_2-HAP treatment group. (d) Two-dimensional PCoA of microbial communities.

significant presence of pathogenic bacteria. Overall, the results suggested that TiO_2-HAP treatment can effectively enhance and safeguard the homeostasis of oral microecology, which is crucial for maintaining oral health.

4 Discussion

Caries and tooth whitening are becoming increasingly concerning.[54–56] However, no materials have been identified that can effectively remove plaque biofilm, promote mineralization, whiten tooth, and maintain the balance of oral flora. To address this issue, we synthesized TiO_2-HAP NPs and investigated its multifunctional properties. Firstly, to select the TiO_2-HAP NPs with optimal performance, we evaluated the titanium-calcium ion molar ratio, synthesis pH conditions, and synthesis time for the NPs. The results indicated that the TiO_2-HAP NPs with a titanium to calcium molar ratio of 1 : 2 exhibited better photocatalytic performance. The addition of HAP may cause a decrease in the original bandgap of TiO_2, this reduction in bandgap lowers the energy required for electron excitation, resulting in an increase in the absorption wavelength. Consequently, the absorption spectrum shifted from the UV range of pure TiO_2 to the blue light spectrum. This shift significantly may enhance the photocatalytic activity of the NPs, and blue light is considered to be more biologically safe compared to UV light.[57] Meanwhile, we found that the synthesized TiO_2-HAP NPs exhibited the most stable morphology and a more uniform distribution of calcium and phosphorus elements when the synthesis pH was set at 11 and the stirring time was 6 h. Additionally, the atomic ratio of the products was more consistent with that of the raw materials. This stability may be attributed to the lower solubility of HAP at pH 11, which facilitates the formation of a stable solid-phase structure.[58] Furthermore, this condition may allow for better control the crystalline phase of TiO_2, resulting in the production of the anatase phase, which is known for its higher photocatalytic activity.[59] It has also been demonstrated that sufficient reaction time ensures adequate mixing of the components in the reaction system.[60] Therefore, we finally choose the TiO_2-HAP NPs with a titanium-to-calcium molar ratio of 1 : 2, a reaction pH of 11, and a reaction time of 6 h for subsequent experiments.

Enamel demineralization occurs in the early stages of caries; however, enamel itself lacks the ability to remineralize and repair. Therefore, in this study, HAP was utilized as

a remineralization agent to enhance the prevention and treatment of early caries. The microhardness of enamel serves as a crucial indicator of the degree of enamel mineralization. The results showed that the differences in microhardness values of enamel were statistically significant ($P < 0.001$), with the exception of the TiO_2-HAP and TiO_2-HAP + LED groups, which indicate that TiO_2-HAP NPs can significantly enhance the microhardness of enamel. However, the hardness of the remineralization products they promote differs from that of normal enamel. The specific composition and structure of these products need to be explored in the future.

Next, the tooth whitening effect of TiO_2-HAP NPs under blue light irradiation was evaluated. The experimental results indicated that after applying TiO_2-HAP NPs and exposing them to blue light irradiation for 10 h, a significant change in tooth color shade was observed. This change was attributed to the fact that TiO_2, as a classical photocatalyst, generates ROS that possess strong oxidative capacity and can effectively decompose organic staining substances.[61] Subsequently, in TiO_2-HAP NPs, HAP can repair microcracks and defects on the tooth surface by interacting with the hydroxyapatite present on the tooth surface and promoting the redeposition of dental minerals. This could not only help enhance the shine of the teeth but also improve the overall appearance of the teeth.[62] A balanced oral microenvironment is essential.[63,64] The results of gene sequencing analyses indicated that three dominant bacteria in the oral microenvironment were not affected by the TiO_2-HAP NPs. The results of PCoA indicated that the TiO_2-HAP treatment group highly overlapped with the negative control group. Additionally, the distribution of the community was more concentrated, suggesting that TiO_2-HAP treatment did not notably disrupt the structure of oral microecological community, and the ecological status was restored to a healthy level. This suggests that the TiO_2-HAP NPs had a beneficial protective effect on the oral microenvironment, which can be attributed to the good biocompatibility and light sensitivity of TiO_2-HAP NPs. Experimenter can determine the antimicrobial range of the treatment by adjusting the area and range of light irradiation. Specifically, the light can be selectively directed onto the bacterial surface of the tooth without disrupting the microenvironmental homeostasis in other regions of the oral cavity, such as the buccal side and the floor of the mouth. This approach is beneficial for the maintenance and protection of oral health.

At the end of the experiment, we established an early caries model of rat mandibular molars and assessed the efficacy of TiO_2-HAP NPs in eliminating biofilm and enhancing mineralization. The results demonstrated that the TiO_2-HAP NPs effectively removed the bacterial biofilm adhered to the tooth surface and inhibited further bacterial erosion of the enamel. Simultaneously, the calcium-to-phosphorus ratio was almost elevated to normal levels, indicating that the mineral components in the enamel were successfully restored. Furthermore, the calcium-to-phosphorus ratio of the molar tooth surface in the prevention group of rats reached 1.80, surpassing the levels observed in the blank control group. This result further confirmed the good efficacy of TiO_2-HAP NPs in preventing early enamel caries. Additionally, the effect to promote enamel mineralization is significantly superior to that observed in the natural state. All of the aforementioned experiments demonstrated the effectiveness of TiO_2-HAP NPs in animal models, indicating that the NPs had good effects on both the treatment and prevention of early enamel caries.

Based on the findings of this study, there is potential for further exploration and development of more efficient and multifunctional photocatalytic-bioceramic composites in the future. For instance, the photocatalytic efficiency of the photocatalytic materials can be enhanced, and their antibacterial and whitening effects can be improved by modulating their crystal structure, particle size, and surface modifications. In addition to TiO_2 and HAP, other functional materials, such as those with anti-inflammatory and antioxidant functions, can be introduced to endow the composites with more biofunctions and enhance their application value in oral disease prevention and treatment. In the subsequent research, more delivery forms suitable for clinical applications, such as gels, coatings, mouthwashes, *etc.*, can be developed.

5 Conclusion

In this study, we successfully synthesized TiO_2-HAP NPs photocatalytic materials to achieve multiple effects, including antibacterial properties, promineralization, and tooth whitening. We first explored the optimal synthesis conditions for TiO_2-HAP, which included a titanium-to-calcium molar ratio of 1 : 2, a reaction pH of 11, and a reaction time of 6 h, and used the TiO_2-HAP for subsequent experiments. The application of TiO_2-HAP NPs significantly improved tooth color through blue light irradiation, resulting in an effective tooth whitening effect. Additionally, TiO_2-HAP NPs demonstrated positive effects in maintaining the balance of the oral microenvironment, did not significantly alter the normal oral flora, and exhibited good *in vivo* biocompatibility. These factors collectively provide strong support for their safety in clinical applications. Finally, we established an early caries model in rats. The experimental results demonstrated that the TiO_2-HAP NPs not only effectively eliminated pathogenic caries bacteria but also enhanced the calcium-to-phosphorus elemental ratio. This finding aligns with the results of *in vitro* microhardness test, confirming its significant ability to promote the remineralization of demineralized tooth enamel. In conclusion, the multifunctional TiO_2-HAP NPs offers a novel approach for the prevention and treatment of early clinical caries.

Data availability

Further data for this research article can be provided as ESI.†

Author Contributions

Ranxu Wang, Yanjiu Wang, Jiayuan Chen and Yue Yin: methodology, validation, investigation, formal analysis, writing – original draft. Nannan Zheng, Mengdi Li, and Shuang Zhao: validation, investigation. Han Xu and Qiwei Li: formal analysis. Yumei Niu, Lin Zhang and Shuang Pan: conceptualization,

project administration, writing – review & editing, funding acquisition, supervision.

Conflicts of interest

There are no conflicts to declare.

Acknowledgements

This work was supported by the Key Project of the Joint Fund of the Natural Science Foundation of Heilongjiang Province, China (No. ZL2024H004); Heilongjiang Provincial Natural Science Foundation of China (Grant No. LH2022H043); Heilongjiang Provincial Key R&D Programme (Grant No. 2022ZX06C05).

References

1 Z. Abedian, N. Jenabian, A. A. Moghadamnia, E. Zabihi, R. Pourbagher and M. Rajabnia, Antibacterial activity of high-molecular-weight and low-molecular-weight chitosan upon oral pathogens, *Int. J. Infect. Dis.*, 2020, **101**, 46–47.

2 M. E. Zarif, S. A. Yehia, B. Bi□ă, V. Sătulu, S. Vizireanu, G. Dinescu, A. M. Holban, F. Marinescu, E. Andronescu, A. M. Grumezescu, A. C. Bîrcă and A. T. Farca□iu, Atmospheric Pressure Plasma Activation of Hydroxyapatite to Improve Fluoride Incorporation and Modulate Bacterial Biofilm, *Int. J. Mol. Sci.*, 2021, **22**, 13103.

3 M. Cao, Z. Qian, Y. Liang, Q. Liu, H. Wang, Y. Meng, Y. Wang and Y. Wang, Layer-by-layer coated probiotics with tannic acid-Ca^{2+} and casein phosphopeptide complexes for caries prevention and enamel remineralization, *IScience*, 2024, **17**, 28.

4 S. A. Rather, S. C. Sharma and A. Mahmood, Antibodies generated against dextransucrase exhibit potential anticariostatic properties in *Streptococcus mutans*, *Appl. Microbiol. Biotechnol.*, 2020, **104**, 1761–1772.

5 H. Wang, S. Wang, L. Cheng, Y. Jiang, M. A. S. Melo, M. D. Weir, T. W. Oates, X. Zhou and H. H. K. Xu, Novel dental composite with capability to suppress cariogenic species and promote non-cariogenic species in oral biofilms, *Mater. Sci. Eng., C*, 2019, **94**, 587–596.

6 K. Sun, W. Wang, X. Wang, X. Shi, Y. Si and S. Zheng, Tooth wear: a cross-sectional investigation of the prevalence and risk factors in Beijing, *BDJ Open*, 2017, **3**, 16012.

7 E. Alhallak, C. Kouchaje, A. Hasan and R. Makieh, Evaluation of the Effectiveness of Probiotic Mouthwashes in Reducing Dental Plaque in Primary and Permanent Teeth: A Randomized Clinical Trial, *Cureus*, 2022, **14**, e28125.

8 K. Janjić and H. Agis, Chronodentistry: the role & potential of molecular clocks in oral medicine, *BMC Oral Health*, 2019, **19**, 1–12.

9 M. Malakootian, M. Javdan and F. Iranmanesh, Use of bauxite from active Iranian mines for the removal of fluoride from drinking water, *Environ. Health Eng. Manage. J.*, 2017, **4**, 217–224.

10 Q. Yu, D. Shao, R. Zhang, W. Ouyang and Z. Zhang, Effects of drinking water fluorosis on L-type calcium channel of hippocampal neurons in mice, *Chemosphere*, 2019, **220**, 169–175.

11 K. Li, S. Chen, J. Wang, X. Xiao, Z. Song and S. Liu, Tooth whitening: current status and prospects, *Odontology*, 2024, **112**, 700–710.

12 B. Gottenbos, C. de Witz, S. Heintzmann, M. Born and S. Hötzl, Insights into blue light accelerated tooth whitening, *Heliyon*, 2021, **7**, e05913.

13 X. Chen, E. B.-M. Daliri, A. Tyagi and D.-H. Oh, Cariogenic Biofilm: Pathology-Related Phenotypes and Targeted Therapy, *Microorganisms*, 2021, **9**, 1311.

14 L. Sedghi, V. DiMassa, A. Harrington, S. V. Lynch and Y. L. Kapila, The oral microbiome: Role of key organisms and complex networks in oral health and disease, *Periodontol*, 2000, **87**, 107–131.

15 Z. Li, Y. Liu and L. Zhang, Role of the microbiome in oral cancer occurrence, progression and therapy, *Microb. Pathog.*, 2022, **169**, 105638.

16 S. Roy, I. Hasan and B. Guo, Recent advances in nanoparticle-mediated antibacterial applications, *Coord. Chem. Rev.*, 2023, **482**, 215075.

17 S. E. Alavi, A. Raza, M. Gholami, M. Giles, R. Al-Sammak, A. Ibrahim, H. Ebrahimi Shahmabadi and L. A. Sharma, Advanced Drug Delivery Platforms for the Treatment of Oral Pathogens, *Pharmaceutics*, 2022, **14**, 2293.

18 L. Zhang, Y.-N. Wu, T. Chen, C.-H. Ren, X. Li and G.-X. Liu, Relationship between intestinal microbial dysbiosis and primary liver cancer, *Hepatobiliary Pancreatic Dis. Int.*, 2019, **18**, 149–157.

19 I. P. Balmasova, E. I. Olekhnovich, K. M. Klimina, A. A. Korenkova, M. T. Vakhitova, E. A. Babaev, L. A. Ovchinnikova, Y. A. Lomakin, I. V. Smirnov, V. N. Tsarev, A. M. Mkrtumyan, A. A. Belogurov, A. G. Gabibov, E. N. Ilina and S. D. Arutyunov, Drift of the Subgingival Periodontal Microbiome during Chronic Periodontitis in Type 2 Diabetes Mellitus Patients, *Pathogens*, 2021, **10**, 504.

20 D. Tang, G. Lu, Z. Shen, Y. Hu, L. Yao, B. Li, G. Zhao, B. Peng and X. Huang, A review on photo-, electro- and photoelectrocatalytic strategies for selective oxidation of alcohols, *J. Energy Chem.*, 2023, **77**, 80–118.

21 L. Yang, D. Fan, Z. Li, Y. Cheng, X. Yang and T. Zhang, A Review on the Bioinspired Photocatalysts and Photocatalytic Systems, *Adv. Sustainable Syst.*, 2022, **6**, 2100477.

22 S. Roy, S. Wang, Z. Ullah, H. Hao, R. Xu, J. Roy, T. Gong, I. Hasan, W. Jiang, M. Li and D. Mondal, Defect-Engineered Biomimetic Piezoelectric Nanocomposites With Enhanced ROS Production, Macrophage Re-polarization, and Ca^{2+} Channel Activation for Therapy of MRSA-Infected Wounds and Osteomyelitis, *Small*, 2025, 2411906.

23 J. Li, X. Wei, Y. Hu, Y. Gao, Y. Zhang and X. Zhang, A fluorescent nanobiocide based on ROS generation for

eliminating pathogenic and multidrug-resistant bacteria, *J. Mater. Chem. B*, 2021, **9**, 3689–3695.

24 A. Verma, S. Shivalkar, M. P. Sk, S. K. Samanta and A. K. Sahoo, Nanocomposite of Ag nanoparticles and catalytic fluorescent carbon dots for synergistic bactericidal activity through enhanced reactive oxygen species generation, *Nanotechnology*, 2020, **31**, 405704.

25 B. Fan, W. Peng, Y. Zhang, P. Liu and J. Shen, ROS conversion promotes the bactericidal efficiency of Eosin Y based photodynamic therapy, *Biomater. Sci.*, 2023, **11**, 4930–4937.

26 A. Melese, W. Wubet, A. Abebe and A. Hussen, A comprehensive review on recent progress in synthesis methods of ZnO/CuO nanocomposites and their biological and photocatalytic applications, *Results Chem.*, 2025, 102141.

27 X. Zhang, S. Zhang, K. Mathivanan, R. Zhang, J. Zhang, Q. Jiang, W. Sand, J. Duan and B. Hou, Research progress and prospects in antifouling performance of photocatalytic sterilization: A review, *J. Mater. Sci. Technol.*, 2025, **208**, 189–201.

28 X. Qi, Z. Zhao, N. Li, Z. He, Y. Chen and T. Jin, Improved photocatalytic and sterilization performance of Cu doped sea urchin-like WO_{3-x}, *New J. Chem.*, 2023, **47**, 3140–3150.

29 J. Guo, J. Zhou, Z. Sun, M. Wang, X. Zou, H. Mao and F. Yan, Enhanced photocatalytic and antibacterial activity of acridinium-grafted g-C_3N_4 with broad-spectrum light absorption for antimicrobial photocatalytic therapy, *Acta Biomater.*, 2022, **146**, 370–384.

30 H. Chakhtouna, H. Benzeid, N. Zari, A. e. k. Qaiss and R. Bouhfid, Recent progress on Ag/TiO_2 photocatalysts: photocatalytic and bactericidal behaviors, *Environ. Sci. Pollut. Res. Int.*, 2021, **28**, 44638–44666.

31 X. Guo, G. Pan, L. Fang, Y. Liu and Z. Rui, Z-Scheme CuOx/Ag/TiO_2 Heterojunction as Promising Photoinduced Anticorrosion and Antifouling Integrated Coating in Seawater, *Molecules*, 2023, **28**, 456.

32 P. Innocenzi and L. Malfatti, Mesoporous ordered titania films: An advanced platform for photocatalysis, *J. Photochem. Photobiol., C*, 2024, **58**, 100646.

33 A. Kompa, M. G. Mahesha, D. Kekuda and M. Rao K, Spectroscopic investigation of defects in spin coated titania based thin films for photocatalytic applications, *J. Solid State Chem.*, 2021, **303**, 122488.

34 L. Zhao, H. Li, Z. Liu, Z. Wang, D. Xu, J. Zhang, J. Ran, H. Mo and L. Hu, Copper ions induces ferroptosis in Staphylococcus aureus and promotes healing of MRSA-induced wound infections, *Microbiol. Res.*, 2025, **25**, 128122.

35 Z. Li, H. Li, Z. Tang, Q. Tang, C. Liao, H. Tang and D. Wang, Design of acidic activation-responsive charge-switchable carbon dots and validation of their antimicrobial activity, *RSC Adv.*, 2025, **15**, 5413–5425.

36 Y.-K. Tao, Y.-W. Tseng, K.-Y. Tzou, C.-Y. Kuo, H. T. Nguyen, H.-T. Lu and A. E. Y. Chuang, Advancing teeth whitening efficacy via dual-phototherapeutic strategy incorporating molybdenum disulfide embedded in carrageenan hydrogel for dental healthcare, *Int. J. Biol. Macromol.*, 2024, **276**, 133647.

37 X. Liu, R. Qian, B. Li, Y. Zhang and Y. Han, Sono-Catalytic Tooth Whitening and Oral Health Enhancement with Oxygen Vacancies-Enriched Mesoporous TiO_2 Nanospheres: A Nondestructive Approach for Daily Tooth Care, *ACS Biomater. Sci. Eng.*, 2024, **10**, 6634–6647.

38 Z. Mai, D. Liu, Z. Chen, D. Lin, W. Zheng, X. Dong, Q. Gao and W. Zhou, Fabrication and Application of Photocatalytic Composites and Water Treatment Facility Based on 3D Printing Technology, *Polymers*, 2021, **13**, 2196.

39 D. Athanasiadou, A. L. Danesi, L. Umbrio, J. Holcroft, B. Ganss and K. M. M. Carneiro, Hydroxyapatite Growth on Amelogenin–Amelotin Recombinamers, *ChemNanoMat*, 2021, **7**, 851–857.

40 A. L. Danesi, D. Athanasiadou, A. Mansouri, A. Phen, M. Neshatian, J. Holcroft, J. Bonde, B. Ganss and K. M. M. Carneiro, Uniaxial Hydroxyapatite Growth on a Self-Assembled Protein Scaffold, *Int. J. Mol. Sci.*, 2021, **22**, 12343.

41 D. Zhang, J. Guo, S. Li, Y. Pang, Y. Yu, X. Yang and Q. Cai, A resin adhesive with balanced antibacterial and mineralization properties for improved dental restoration, *Int. J. Adhes. Adhes.*, 2023, **126**, 103469.

42 B. Maheshwaran, J. Chokkatt, A. Shenoy, D. Ganapathy, P. Yadalam and M. Marrapodi, Therapeutic evaluation of titanium dioxide nanoparticles based herbal dental varnish derived from rosemary and ginger extracts:a comprehensive investigation into anti-inflammatory and antioxidant properties, *Technol. Health Care.*, 2024, **32**, 2783–2792.

43 M. Ji, G. Oh, J. Kim, S. Park, K. Yun, J. Bae and H. Lim, Effects on Antibacterial Activity and Osteoblast Viability of Non-Thermal Atmospheric Pressure Plasma and Heat Treatments of TiO_2 Nanotubes, *J. Nanosci. Nanotechnol.*, 2017, **17**, 2312–2315.

44 R. Shirai, T. Miura, A. Yoshida, F. Yoshino, T. Ito, M. Yoshinari and Y. Yajima, Antimicrobial effect of titanium dioxide after ultraviolet irradiation against periodontal pathogen, *Dent. Mater. J.*, 2016, **35**, 511–516.

45 N. Monteiro, R. Basting, F. Amaral, F. França, C. Turssi, O. Gomes and R. Basting, Titanium dioxide nanotubes incorporated into bleaching agents: physicochemical characterization and enamel color change, *J. Appl. Oral Sci.*, 2020, **28**, e20190771.

46 A. Weir, P. Westerhoff, L. Fabricius, K. Hristovski and N. Von Goetz, Titanium dioxide nanoparticles in food and personal care products, *Environ. Sci. Technol.*, 2012, **46**, 2242–2250.

47 M. Shakir, H. Mohammed-Salih, F. Hussein, J. Al-Obaidi and F. Supian, Innovation of nano-hydrogels loaded with amelogenin peptide and hydroxyapatite nano-particles for remineralisation of artificially induced white spot lesions, *J. Drug Delivery Sci. Technol.*, 2024, **99**, 105986.

48 R. Wang, C. Jia, N. Zheng, S. Liu, Z. Qi, R. Wang, L. Zhang, Y. Niu and S. Pan, Effects of photodynamic therapy on Streptococcus mutans and enamel remineralization of

multifunctional TiO_2-HAP composite nanomaterials, *Photodiagn. Photodyn. Ther.*, 2023, **42**, 103141.

49 H. Ohno, M. Hashimoto, Y. Araki, T. Nezu and K. Endo, Chemical interaction of 4-META with enamel in resin-enamel bonds, *Dent. Mater. J.*, 2021, **40**, 683–688.

50 N. Linh, P. Tuan and N. Dzung, The shifts of band gap and binding energies of titania/hydroxyapatite material, *J. Compos.*, 2014, **2014**, 283034.

51 S. Arunmetha, N. Dhineshbabu, A. Kumar and R. Jayavel, Preparation of sulfur doped TiO_2 nanoparticles from rutile sand and their performance testing in hybrid solar cells, *J. Mater. Sci.: Mater. Electron.*, 2021, **32**, 28382–28393.

52 S. Kareiva, V. Klimavicius, A. Momot, J. Kausteklis, A. Prichodko, L. Dagys, F. Ivanauskas, S. Sakirzanovas, V. Balevicius and A. Kareiva, Sol-gel synthesis, phase composition, morphological and structural characterization of $Ca_{10}(PO_4)_6(OH)_2$: XRD, FTIR, SEM, 3D SEM and solid-state NMR studies, *J. Mol. Struct.*, 2016, **1119**, 1–1.

53 A. Mitsionis, T. Vaimakis, C. Trapalis, N. Todorova, D. Bahnemann and R. Dillert, Hydroxyapatite/titanium dioxide nanocomposites for controlled photocatalytic NO oxidation, *Appl. Catal., B*, 2011, **106**, 398–404.

54 Z. Abedian, N. Jenabian, A. A. Moghadamnia, E. Zabihi, R. Pourbagher and M. Rajabnia, Antibacterial activity of high-molecular-weight and low-molecular-weight chitosan upon oral pathogens, *J. Conservative Dent.*, 2020, **101**, 46–47.

55 M. E. Zarif, S. A. Yehia, B. Bi□ă, V. Sătulu, S. Vizireanu, G. Dinescu, A. M. Holban, F. Marinescu, E. Andronescu, A. M. Grumezescu, A. C. Bîrcă and A. T. Farca□iu, Atmospheric Pressure Plasma Activation of Hydroxyapatite to Improve Fluoride Incorporation and Modulate Bacterial Biofilm, *Int. J. Mol. Sci.*, 2021, **22**, 13103.

56 Y. Wang, X. Wen, Y. Jia, M. Huang, F. Wang, X. Zhang, Y. Bai, G. Yuan and Y. Wang, Piezo-catalysis for nondestructive tooth whitening, *Nat. Commun.*, 2020, **11**, 1328.

57 T. Sugiyama and Y. Chen, Biochemical reconstitution of UV-induced mutational processes, *Nucleic Acids Res.*, 2019, **47**, 6769–6782.

58 I. Fernando and Y. Zhou, Impact of pH on the stability, dissolution and aggregation kinetics of silver nanoparticles, *Chemosphere*, 2019, **216**, 297–305.

59 S. Kment, F. Riboni, S. Pausova, L. Wang, L. Wang, H. Han, Z. Hubicka, J. Krysa, P. Schmuki and R. Zboril, Photoanodes based on TiO_2 andα-Fe_2O_3 for solar water splitting–superior role of 1D nanoarchitectures and of combined heterostructures, *Chem. Soc. Rev.*, 2017, **46**, 3716–3769.

60 Y. Xie, S. Lyu, Y. Zhang and C. Cai, Adsorption and Degradation of Volatile Organic Compounds by Metal–Organic Frameworks (MOFs): A Review, *Materials*, 2022, **15**, 7727.

61 Y. Kowaka, K. Nozaki, T. Mihara, K. Yamashita, H. Miura, Z. Tan and S. Ohara, Development of TiO_2 Nanosheets with High Dye Degradation Performance by Regulating Crystal Growth, *Materials*, 2023, **16**, 1229.

62 A. Butera, C. Maiorani, S. Gallo, M. Pascadopoli, M. Quintini and M. Lelli, Biomimetic action of zinc hydroxyapatite on remineralization of enamel and dentin: a review, *Biomimetics*, 2023, **8**, 71.

63 I. P. Balmasova, E. I. Olekhnovich, K. M. Klimina, A. A. Korenkova, M. T. Vakhitova, E. A. Babaev, L. A. Ovchinnikova, Y. A. Lomakin, I. V. Smirnov, V. N. Tsarev, A. M. Mkrtumyan, A. A. Belogurov, A. G. Gabibov, E. N. Ilina and S. D. Arutyunov, Drift of the Subgingival Periodontal Microbiome during Chronic Periodontitis in Type 2 Diabetes Mellitus Patients, *Pathogens*, 2021, **10**, 504.

64 H. Lv Pan, F. Zhang, S. Chen, Y. Cheng, S. Ma, H. Hu, X. Liu, X. Cai, F. Fan and S. Gong, Green tea extracts alleviate acetic acid-induced oral inflammation and reconstruct oral microbial balance in mice, *J. Food Sci.*, 2023, **88**, 5291–5308.